Comparison of Manual and Object-Based Delineation for Aerial Image Interpretation

Amy Reinert, Daniel Rokitnicki-Wojcik, and Jonathan Midwood

Great Lakes Laboratory for Fisheries and Aquatic Sciences
Science Branch, Ontario and Prairie Region
Fisheries and Oceans Canada
867 Lakeshore Road, Burlington, ON, L7S1A1

2022

Canadian Technical Report of
Fisheries and Aquatic Sciences 3493

Fisheries and Oceans Canada | Pêches et Océans Canada

Canada

Canadian Technical Report of Fisheries and Aquatic Sciences

Technical reports contain scientific and technical information that contributes to existing knowledge but which is not normally appropriate for primary literature. Technical reports are directed primarily toward a worldwide audience and have an international distribution. No restriction is placed on subject matter and the series reflects the broad interests and policies of Fisheries and Oceans Canada, namely, fisheries and aquatic sciences.

Technical reports may be cited as full publications. The correct citation appears above the abstract of each report. Each report is abstracted in the data base *Aquatic Sciences and Fisheries Abstracts*.

Technical reports are produced regionally but are numbered nationally. Requests for individual reports will be filled by the issuing establishment listed on the front cover and title page.

Numbers 1-456 in this series were issued as Technical Reports of the Fisheries Research Board of Canada. Numbers 457-714 were issued as Department of the Environment, Fisheries and Marine Service, Research and Development Directorate Technical Reports. Numbers 715-924 were issued as Department of Fisheries and Environment, Fisheries and Marine Service Technical Reports. The current series name was changed with report number 925.

Rapport technique canadien des sciences halieutiques et aquatiques

Les rapports techniques contiennent des renseignements scientifiques et techniques qui constituent une contribution aux connaissances actuelles, mais qui ne sont pas normalement appropriés pour la publication dans un journal scientifique. Les rapports techniques sont destinés essentiellement à un public international et ils sont distribués à cet échelon. II n'y a aucune restriction quant au sujet; de fait, la série reflète la vaste gamme des intérêts et des politiques de Pêches et Océans Canada, c'est-à-dire les sciences halieutiques et aquatiques.

Les rapports techniques peuvent être cités comme des publications à part entière. Le titre exact figure au-dessus du résumé de chaque rapport. Les rapports techniques sont résumés dans la base de données *Résumés des sciences aquatiques et halieutiques.*

Les rapports techniques sont produits à l'échelon régional, mais numérotés à l'échelon national. Les demandes de rapports seront satisfaites par l'établissement auteur dont le nom figure sur la couverture et la page du titre.

Les numéros 1 à 456 de cette série ont été publiés à titre de Rapports techniques de l'Office des recherches sur les pêcheries du Canada. Les numéros 457 à 714 sont parus à titre de Rapports techniques de la Direction générale de la recherche et du développement, Service des pêches et de la mer, ministère de l'Environnement. Les numéros 715 à 924 ont été publiés à titre de Rapports techniques du Service des pêches et de la mer, ministère des Pêches et de l'Environnement. Le nom actuel de la série a été établi lors de la parution du numéro 925.

Canadian Technical Report of
Fisheries and Aquatic Sciences 3493

2022

Comparison of Manual and Object-Based Delineation for Aerial Image Interpretation

by

Amy Reinert[2,3], Daniel Rokitnicki-Wojcik[2,4], and Jonathan D. Midwood[1]

[1]Great Lakes Laboratory for Fisheries and Aquatic Sciences
Science Branch, Ontario and Prairie Region
Fisheries and Oceans Canada
867 Lakeshore Road
Burlington ON, L7S 1A1

[2] Canadian Wildlife Service – Ontario Region
Environment and Climate Change Canada
4905 Dufferin St.
Toronto, ON M3H 5T4

[3] Current Address: Natural Resources Solutions Inc.
415 Philip St. Unit C
Waterloo ON, N2L 3X2

[4]Current Address: Environment and Climate Change Canada
867 Lakeshore Road
Burlington ON, L7S 1A1

Cat. No. Fs97-6/3493E-PDF ISBN 978-0-660-44179-5 ISSN 1488-5379

Correct citation for this publication:
Reinert, A., Rokitnicki-Wojcik, D., and Midwood, J.D. 2022. Comparison of manual and object-based delineation for aerial image interpretation. Can. Tech. Rep. Fish. Aquat. Sci. 3493: vi + 36 p.

TABLE OF CONTENTS

LIST OF TABLES AND FIGURES

ABSTRACT

Reinert, A., Rokitnicki-Wojcik, D., and Midwood, J.D. 2022. Comparison of manual and object-based delineation for aerial image interpretation. Can. Tech. Rep. Fish. Aquat. Sci. 3493: vi + 36 p.

Habitat management and landscape assessment often require the interpretation of aerial or satellite images for the identification of land cover classes. This involves delineating the boundaries of features with similar characteristics and assigning a class (e.g., vegetation, water, structures). Historically, manual delineation by an interpreter was the primary method used, but more recently object-based methods that use pre-defined segmentation parameters to divide an image into polygons with similar characteristics are increasing in popularity. Here we compare the accuracy and efficiency (in terms of effort) of the object-based method with manual delineation. We use aerial imagery from Big Creek National Wildlife Area, Lake Erie collected in 2006. Ten image subsets were manually digitized and segmented using the object-based method and then all polygons were classified as one of nine land cover types. While the manual and object-based methods yielded classifications with comparable overall accuracy (91% and 90%, respectively), the object-based method was significantly more efficient, requiring approximately half as much time to complete the interpretation of image subsets. Key advantages of the object-based approach were its ability to delineate feature boundaries more precisely than the manual method by limiting digitizing errors and its potential to reduce differences from multiple interpreters. It is recommended that object-based segmentation be used to aid in the interpretation and classification of land cover classes in aerial and satellite imagery.

RÉSUMÉ

Reinert, A., Rokitnicki-Wojcik, D., and Midwood, J.D. 2022. Comparison of manual and object-based delineation for aerial image interpretation. Can. Tech. Rep. Fish. Aquat. Sci. 3493: vi + 36 p.

La gestion de l'habitat et l'évaluation du paysage exigent souvent l'interprétation d'images aériennes ou satellitaires pour la détermination des catégories de couverture terrestre. Pour ce faire, on doit délimiter les entités ayant des caractéristiques similaires et leur attribuer une classe (p. ex. la végétation, l'eau, les structures). Historiquement, la délimitation manuelle par un interprète était la principale méthode utilisée, mais plus récemment, les méthodes basées sur des objets qui utilisent des paramètres de segmentation prédéfinis pour diviser une image en polygones ayant des caractéristiques similaires gagnent en popularité. Nous comparons ici la précision et l'efficacité (en termes d'effort) de la méthode basée sur des objets avec la délimitation manuelle. Nous avons utilisé des images aériennes de la réserve nationale de faune de Big Creek, sur les rives du lac Érié, prises en 2006. Dix sous-ensembles d'images ont été numérisés manuellement et segmentés à l'aide de la méthode basée sur des objets, puis tous les polygones ont été classés comme l'une de neuf catégories de couverture terrestre. Bien que la méthode manuelle et la méthode basée sur des objets aient permis d'obtenir des classifications avec une précision globale comparable (91 % et 90 %, respectivement), la méthode basée sur des objets s'est avérée beaucoup plus efficace, ne demandant environ que la moitié du temps nécessaire pour effectuer l'interprétation des sous-ensembles d'images. Les principaux avantages de l'approche basée sur des objets étaient sa capacité à définir les limites des caractéristiques avec plus de précision que la méthode manuelle en limitant les erreurs de numérisation et sa capacité à réduire les différences entre plusieurs interprètes. Il est donc recommandé d'utiliser la segmentation basée sur des objets pour faciliter l'interprétation et la classification des catégories de couverture terrestre dans l'imagerie aérienne et satellitaire.

INTRODUCTION

Aerial or satellite imagery are routinely used in environmental management to help map areas and features of interest, quantify their coverage, and track changes in feature type and cover through time (Pettorelli et al. 2016; Dauwalter et al. 2017; Marcaccio et al. 2021). Its importance to management has driven the development of new methods of interpretation aiming to increase accuracy and efficiency (Morgan et al. 2010). The manual interpretation of aerial images, which consists of manual polygon delineation and classification by an interpreter, is one of the most commonly used methods for producing thematic maps of tangible information (Wulder 1998; Thompson et al. 2007). In this method, characteristics such as colour, shape, size, texture, pattern and neighbouring contextual cues are used to delineate the polygon boundaries of features with similar properties (Morgan and Gergel 2013). While historically manual delineation has been considered one of the most accurate interpretation methods (Wulder 1998), there are several disadvantages of this method. Because the manual delineation of features relies on the skill and knowledge of the interpreter, the resulting thematic maps are subjective and can be vulnerable to errors and inconsistencies (e.g., inconsistent assignment of class types, invalid geometry, different edge delineation by different analysts; Thompson et al. 2007; Wulder et al. 2008; Morgan et al. 2010). Manual interpretation can also be labour intensive, time consuming, and expensive (Pringle et al. 2009; Morgan and Gergel 2013).

Due to the importance and widespread use of aerial image interpretation and in order to resolve some of the issues encountered with the traditional manual approach, several automated methods of feature delineation have been developed. Historically, automatic image segmentation relied on a pixel by pixel analysis where computer algorithms delineated each pixel of a digital image. This method, however, only produces accurate results if the image pixel sizes remain finer than the objects of interest that are being delineated (Blaschke 2010). Furthermore, this method splits the image into square units, which is not accurate or relevant for features that are not rectangular in shape and therefore often results in low classification accuracies (Burnett and Blaschke 2003; Pringle et al. 2009; Blaschke 2010). Object-based image segmentation and analysis, wherein neighbouring pixels are grouped into objects based on similar characteristics and contextual information about the properties of other objects in the image (Benz et al. 2004), is now available in a variety of remote sensing software [e.g. eCognition Developer (Trimble Geospatial, California, USA); ENVI (Harris Geospatial, Colorado, USA); PCI Geomatica (PCI Geomatics, Markham, ON); ArcPro (ESRI, California, USA)]. This process automatically segments the image into non-overlapping units (similar to delineated polygons) based on the user defined parameters for scale (minimum or maximum size of the polygon allowed), colour (importance of spectral properties in the grouping of like pixels), texture (homogeneity of the encapsulated pixels), shape (importance of the ultimate shape of the final polygon in grouping like pixels), and neighbourhood (connectivity and proximity to other objects). Once determined, the appropriate segmentation parameters can be readily applied to other images of a similar type and containing similar land cover, facilitating the consistent

comparison of data from different sources and over time. This image segmentation process is analogous to the process of manually digitizing the boundary of polygons and, after both processes, derived polygons can be manually or automatically classified as land cover classes of interest.

There are many successful uses of the object-based segmentation processes in the literature (e.g., Grenier et al. 2008; Midwood and Chow-Fraser 2010; Pande-Chhetri et al. 2017), but few studies have actually compared the classification results of manual delineation and object-based segmentation (Blaschke 2010). The few existing studies do, however, indicate promising results, with object-based segmentation typically having similar accuracies as traditional manual delineation. Specifically, Morgan and Gergel (2013) found that over 70% of the characteristics of automatically segmented and classified objects were statistically similar to that of manually delineated and classified polygons. Kampouraki et al. (2007) found an overall agreement of 92% between the manual delineation and object-based segmentation methods. Finally, Zhou and Troy (2008) compared object-based segmentation and classification to a manually delineated reference map, which resulted in an overall accuracy of 92%. These studies all suggest that the object-based method has the potential to replace the traditional method of manual delineation for aerial image interpretation. To our knowledge, however, no studies have paired an evaluation of the efficiency of the two interpretation methods with classification accuracy assessments. Determining method efficiency is an essential component for comparison because, if the interpretation methods are equally accurate, the more efficient method should be used.

The goals of this study were to compare the accuracy and efficiency of object-based segmentation and manual delineation for classifying land cover types in Big Creek National Wildlife Area. This comparison focused on the segmentation and delineation component of the image interpretation process, as both methods involve the creation and manual or automated classification of features. If results indicate that object-based segmentation is equally accurate and more efficient than manual delineation, automated techniques should become the method of choice when interpretation is deemed necessary. The replacement of the traditional method of manual delineation with a more efficient and equally accurate object-based method would result in the more efficient use of aerial and satellite imagery, saving valuable time and resources for management agencies.

METHODS

STUDY SITE

This analysis was conducted using imagery of the Big Creek Unit of Big Creek National Wildlife Area, located on the north shore of Lake Erie near Port Rowan, Ontario (Figure 1). This National Wildlife Area consists mainly of wetland habitat and consequently, the majority of classes delineated represent wetland habitat types (discussed below). Aerial imagery from the 2006 Southwestern Ontario Orthophotography Project (SWOOP) was used for this study, which has a pixel resolution of 30 cm. This imagery was selected

because it was deemed to provide sufficient resolution to delineate the proposed wetland land classes. The study area was divided into ten 21-hectare subsets which were spaced equally throughout the study area (Figure 2). Before the testing subsets were interpreted, two additional, spatially distinct training subsets were analyzed using both manual delineation and object-based segmentation. These pilot areas were used to allow the interpreter an opportunity to practice digitizing in each of the software programs and to help them become more familiar with the appearance of the specific land cover classes that are found within the study area.

MANUAL DELINEATION

The ten image subsets were manually delineated using ArcGIS software (version 10.3; ESRI, Redlands, CA). Polygons representing areas of uniform land cover were manually digitized and subsequently classified by manual interpretation. Digitization occurred at a scale of 1:1000, which is the scale used for Ecological Land Classification (ELC) mapping in Ontario by the Canadian Wildlife Service of Environment and Climate Change Canada (Lee et al. 1998). Polygons less than 150 m^2, like those found in highly heterogeneous patches of emergent vegetation or those comprising a single tree, were omitted due to the increased time and effort required for manual delineation. The time required for the delineation of each subset from the start of image editing to the completion of polygon classification and merging was recorded.

OBJECT-BASED SEGMENTATION

The ten image subsets were automatically segmented using eCognition Developer 8.9 (Trimble, Sunnyvale, CA). Each subset image was automatically segmented with input segmentation parameters set at a scale of 75 with a shape of 0.1 and compactness of 0.5 (all unit-less parameters in this software). These parameters were deemed to be appropriate for accurately segmenting the study image into land cover types of interest based on the application of different parameters to the two original pilot areas (data not shown). After segmentation, each image was manually classified using the manual editing tool zoomed to a level of 100%, which is similar to the scale used for manual delineation. In each subset, objects from the same class were merged into one polygon using a loop function and the completed polygons were then exported into ArcGIS for further analysis. The time required for the segmentation of each subset from the start of the automatic image segmentation process until the polygons were imported into ArcGIS was recorded.

LAND COVER CLASSES

All polygons in each of the ten subsets were manually classified for both methods. To avoid any bias, the method used first when completing each subset was alternated. For example, subset one was interpreted using the manual method and then the object-based method while subset two was interpreted using the object-based method and then the manual method. The interpretation of a subset using both methods was completed consecutively in the same day to retain consistent identification of classes.

Nine land cover classes were used for this analysis (Table 1): shallow marsh (MA), two marsh sub-types that represent shallow marshes dominated by cattails (*Typha* sp; CMA) or bulrush marsh (*Schoenoplectus* sp.; BMA), mixed meadow (MME), open water (Water), shallow water with emergent aquatic vegetation (ESA), shallow water with floating aquatic vegetation (FSA), Phragmites species (PHG – which predominately represents non-native common reed; *Phragmites australis*, subsp. *australis;* herein Phragmites) and a class for all other land cover types (Other) – typically representing forest.

Land cover classes were based on those outlined in the ELC for Southern Ontario (Lee et al. 1998) with some important differences. Differences between the classes used in the present study and the ELC reflect the inability of the interpreter to determine substrate type and verify classes in the field or with ground truth data collected at the time of image acquisition. As a result, for several classes, different codes are used than what is typically used for ELC mapping (Table 1).

COMPARISON OF METHOD RESULTS

The efficiency of each method was analyzed by comparing the total time required to complete the interpretation of each subset using each method. Time was recorded in seconds but converted to decimal minutes for easier presentation of results. Analyses were conducted using a paired t-test in R 3.2.0 (R Core Team 2020). In addition, the number of cursor clicks (vertices) required to delineate polygons using the manual method and the number of cursor clicks required to classify objects with the object-based method for each subset were also compared using a paired t-test in R.

To compare the accuracy of classifications using each method, 100 random points were generated within each of the ten subsets using ArcGIS (for 1000 points in total). Each random point (herein referred to as “reference points”) was assigned the “correct” land cover classification by the interpreter; this assignment was done first and without input from either the manual or object-based classification. Confusion matrices were used to determine the accuracy of land cover classifications by comparing the classifications assigned by each method with the correct classification at each reference point. User and producer accuracies were calculated for each method. The producer accuracy relates to the probability that a reference point will be correctly classified and measures the errors of omission. The user accuracy indicates the probability that a classified polygon is representative of the true classification and measures the error of commission or inclusion (Congalton 1991). The accuracy for each subset was compared between methods using a paired t-test.

The total area of each subset that was classified into each land cover class was also compared to determine which classes were being consistently or inconsistently classified between the two methods. Total area was analyzed because classes that are not dominant may have fewer corresponding reference points, which may result in lower user and producer accuracies. Confusion matrices were used to compare the proportional area of overlap between the two methods, which represents the total area

of each subset classified as each land cover class that the methods classified in agreement.

RESULTS

COMPARISON OF TIME REQUIRED

The total time required to complete the interpretation of each image subset was recorded for both methods (Table 2). For the manual delineation method this time period included all steps until polygons were classified and for the object-based segmentation method all steps until images were imported into ArcGIS were timed. The mean time to complete the segmentation and classification of each 21 ha image subset was 55 ± 18 minutes for the manual method and 28 ± 10 minutes for the object-based method. This was calculated by converting recorded times into minutes and averaging the values over all subsets. The time required to interpret a subset using the manual method was significantly longer than the time required to interpret a subset using the object-based method (paired t-test, $t_{(9)} = 8.30$, $p < 0.0001$).

The total time required to interpret images of various sizes, assuming similar complexity and landscapes, were predicted for each method using the rate of interpretation observed in this study. The average rates of interpretation were approximately 23.5 and 45.3 ha per hour for the manual and object-based methods, respectively (Figure 3).

COMPARISON OF CLICK COUNTS

To further compare the efficiency of the two interpretation methods, the number of cursor clicks required to interpret a subset using the manual delineation and object-based segmentation methods was compared (Table 3). The number of cursor clicks required to interpret a subset using the manual method was significantly higher than the object-based method, with 8853 ± 3142 and 634 ± 123 cursor clicks, respectively (paired t-test, $t_{(9)} = -8.34$, $p < 0.0001$). The number of vertices in final polygons created by each method was also compared to analyze polygon complexity (Table 3). Polygons created by the object-based method had 5.2 times the mean number of vertices as manually created polygons (i.e., the object-based derived polygons were more “complex”).

COMPARISON OF METHOD ACCURACY

The accuracy of each method was determined by comparing the user assigned polygon classifications to the classifications of 100 random reference points that were generated within each subset. The overall classification agreement of each interpretation method with the reference points was fairly high, ranging from 87 – 94% (mean = 91% ± 3%; Table 4) for the manual delineation method and from 82 – 95% (mean = 90% ± 3%; Table 4) for the object-based segmentation method. The overall agreement of each method with the reference points was not significantly different between the two methods for within subsets (paired t-test, $t_{(9)} = 0.68$, $p > 0.05$).

Confusion matrices were produced to determine the user and producer accuracy for the interpretation of subsets by each method (Appendix A). The user and producer accuracy for each land cover class was analyzed to determine which classes were most often correctly classified or misclassified using each method (Table 5). The CMA land cover class had a relatively low accuracy for both classification methods, with mean user accuracies of 58% and 72% for manual and object-based delineation, respectively. Similarly, the BMA class also had a relatively low mean user accuracy of 54% for the manual method but a higher accuracy of 84% for the object-based method. The FSA class had a mean accuracy of only 56% for the manual method but was accurate 100% of the time for object-based method. It should be noted, however, there were only three random reference points in one image subset that were classified as FSA. The mean user accuracy for the PHG class was 81% for the manual method but only 50% for the object-based method; however, the PHG class also had limited reference points (seven spread across only four of the ten image subsets). The “other” land class was 100% accurate for both methods, likely because there were only three random reference points across all ten subsets that were classified as other. The most accurate classifications were for water, with user accuracies of 94% for the manual method and 100% for the object-based method. The producer accuracy was similar between methods for six of the nine classes and was slightly higher for the manual MME and FSA classifications and lower for the manual PHG classifications (Table 5).

COMPARISON OF CLASS AREA

To compare the classification results of the two methods, the total area of a subset classified as each land cover type was compared between methods. The proportional area of overlap, which represents the proportion of each subset in which the two methods classified land cover types in agreement, was calculated using confusion matrices of the total area classified as each land cover type (Appendix B). For example, the total area classified as MA by the manual method was compared with the total area classified as MA by the object-based method. The proportional area of overlap is the proportion of the total area classified as MA by the manual method that both methods had classified as MA and indicates whether the two methods classified a similar total area for each land cover type. Generally, the two methods produced similar classification results (Figure 4). The MME and BMA land cover types had relatively low proportional overlap for all image subsets suggesting that the two methods did not consistently classify these land cover types; this is further supported by generally low accuracy for BMA for both methods. By comparison, the MA and water classifications typically had the highest proportional area of overlap between the two methods suggesting that the two methods consistently classified these land cover types. Subsets 1 and 2 contained a combined total of eight polygons that were assigned a classification using one method (mostly object-based) but not the other. Because these polygons were no larger than 0.28 m^2 and totalled 0.85 m^2 in size they can likely be attributed to manual digitizing error. These were the first polygons digitized, suggesting that unfamiliarity with the program may have contributed to the presence of these errors and increased use may have led to a better understanding of the tools available for subsequent subsets.

DISCUSSION

The manual delineation method of aerial image interpretation required significantly more time for interpretation than the object-based segmentation method. The manual method requires the interpreter to manually delineate the boundaries of polygons with similar features, which is indicated by the significantly higher number of cursor clicks required, while this is done automatically with a few cursor clicks in the object-based method. The mean number of cursor clicks required to complete a subset using the manual method was 14 times the mean number of cursor clicks required using the object-based method. Cursor clicks can be used as an approximation of interpreter effort to complete image interpretation and lower click counts represent reduced exposure to the repeated stresses associated with using a cursor. This suggests that the object-based method would be beneficial by reducing the potential for repetitive stress associated with digitizing.

The time required for the eCognition software to segment the image was negligible (typically less than one minute) and exporting polygons to ArcMap only took a matter of seconds (Appendix C). Newer versions of GIS software (e.g., ArcPro, ESRI, Redlands, CA) offer object-based segmentation options that will negate the need to transfer polygons between software. The delineation of polygons was the most time intensive component of the manual method and classification required the most time for the object-based method. With a significantly faster rate of interpretation, almost double that of the manual method, the use of the object-based method would save significant time and resources when interpreting aerial imagery. Because both interpretation methods were equally accurate (based on the overall classification agreement between reference points and the assigned classifications), the object-based method is an acceptable alternative to the more time consuming manual delineation method. Despite the methods being equally accurate, there were differences between the classification results produced by each method.

The user accuracy for image interpretation was analyzed to determine which land cover classes were most often correctly classified (indicated by high user accuracy) or misclassified (indicated by low user accuracy) by each method. CMA had relatively low user accuracy when classified by both methods and BMA had low user accuracy only when classified by the manual method. These land cover types have a characteristic interspersed speckled pattern across the landscape and consist of many small, irregularly shaped patches (Figure 5). The manual method used here only attempted to delineate polygons of a certain size (>150m^2) because the delineation of smaller features would have been time prohibitive for an already time intensive method. The higher user accuracy for BMA with the object-based method likely occurred because this method does not have the same type of minimum polygon size restrictions (i.e., minimum size that a user can accurately manually delineate) and can thus delineate smaller features than the manual method. While setting a minimum polygon size for manual digitizing was necessary, it comes with a trade-off of reduced accuracy for land cover classes that are present in small heterogeneous patches (such as CMA and BMA). Since reference points were randomly generated *a priori*, it is possible that some points ended up in these smaller patches that were not manually digitized and

contributed to reduced accuracy. This may have slightly reduced class-specific accuracies for the manual method; however, it likely had a limited impact on overall accuracies since most land cover types were present in large and more homogenous patches.

The object-based method was able to define polygon boundaries more precisely than the manual method, which, by comparison, created more imprecise boundaries that were created with fewer vertices or clicks by the interpreter. Greater polygon complexity is typical for natural features since they are less likely to be described by simple shapes as would be expected in more linear anthropogenic features (e.g., roads or buildings). The higher number of vertices in polygons created by the object-based method therefore indicates significantly more complex polygons and boundaries. We presume, therefore, that increased complexity resulted in more precise boundaries between features defined using objects than those defined using the manual method; this greater boundary precision would similarly contribute to higher user accuracies for some land cover types (Figure 5).

CMA was most often misclassified as BMA or MA (of which both CMA and BMA are sub-categories) and occasionally water. BMA misclassifications may result from the noted interspersed speckled pattern of the two classes, which may have caused several patches of different land classes to be grouped into the same polygon in the manual method. The misclassifications as MA or water may be explained by the proximity of CMA to these classes. CMA was often found along the water's edge or surrounded by MA, which may indicate that imprecise boundary delineations from the manual method may result in the entire feature not being correctly delineated and therefore, being partially misclassified. Several of the CMA polygons created by the object-based method were fairly small and irregular in shape, and were typically surrounded by other land classes making differentiating objects and classifying them difficult. Similarly, BMA was most often misclassified as MA or CMA, classes that were typically found surrounding BMA patches. These common misclassifications have most likely also resulted from the speckled nature of the land classes and imprecise boundary delineation.

The user accuracy for the PHG land classification was relatively low for the object-based method. The low user accuracy for this class may be partially attributed to reference points, given that only seven of 1,000 reference points were classified as PHG. However, one of the disadvantages of the object-based method is that it does not have the ability to make logical decisions when delineating feature boundaries. The program determines a feature's boundary based on the characteristics, such as texture and colour, and the contextual cues of neighbouring pixels but cannot duplicate the experience of a trained interpreter. For example, an interpreter would know that Phragmites patches are typically round and would therefore digitize Phragmites patches as relatively round polygons (Jung et al. 2017). While the eCognition program can incorporate the shape of features into its delineation of objects, in the present study, shape was not assigned a high weight (only 0.1 out of a maximum of 1.0). Consequently, feature shape was likely overridden by similarities in the colour or texture of neighbouring pixels (Figure 6). Phragmites was most often misclassified as MA,

which was typically found surrounding Phragmites patches, indicating that misclassifications were mostly a result of incorrect boundary delineation. In order to improve PHG differentiation using the object-based method, the input segmentation parameters can be altered to increase the importance of shape in the initial creation of objects. In some software, such as eCognition, a hierarchical image segmentation approach could be used to classify features with such distinct shape parameters and then classify other features based primarily on texture and colour. The goals of each project and study area used will dictate the segmentation parameters that are chosen. This additional step in the object segmentation process will need to be determined using an iterative approach and will thus require additional time. However, once the appropriate segmentation parameters are determined for features of interest, they can be directly applied to other images with similar land cover types and specifications. An additional step that could resolve potential errors in object creation would be for an interpreter to visually inspect automatically segmented images in order to identify and edit any incorrect image segmentations or alter the segmentation parameters and re-run the segmentation before data are used for further analyses. While this would add more time to the overall process, it likely would still not be as time consuming as manual delineation with a net gain in overall accuracy.

The water and MA land classes had the highest user accuracies of all the land cover classes, excluding the “other” land class, which only consisted of one correctly classified reference point. The MA land class covered the most land area in the majority of subsets and therefore was likely to have been represented by the majority of random reference points. MA classes also consisted of relatively larger polygons, which would act to decrease the likelihood that a reference point was located close to a feature boundary where classification is more variable due to the blending of land cover types. The water class is a distinct feature and was therefore relatively easy to classify, if not near a feature boundary, which would have resulted in high user accuracies. This class was also found to be easily separated based on the spectral properties of the imagery (see Liu and Yu 2009) and therefore it may be possible to automatically classify this land cover class (and others that are similarly distinct) in the future.

Because the classification of polygons and objects were both assigned manually by the same interpreter, it is not surprising that there are similar total areas for most classes within subsets, regardless of method. The majority of classification disagreements occurred for polygons located on the boundary edges of features due to the different segmentation methods producing different feature boundaries (Figure 7). The area of land within each subset that was classified in agreement between the two methods was highest for the water and MA classifications. As mentioned above, this is likely a result of these classifications occupying the largest area in each subset and water being a distinctive feature that is relatively easy to identify. The MME classification had consistently low proportional area overlap, mostly for the object-based method. Therefore, the manual delineation method classified more area as MME than the object-based method. As mentioned above, the inability of the object-based method to duplicate the experience of an interpreter and perhaps unsuitable image segmentation parameters for all classes may have contributed to misclassifications of long or linear MME pathways that were found throughout the image.

In addition to the efficiency and boundary precision advantages of the object-based method identified in this analysis, there are several other features of this method that may increase its popularity for use in aerial image interpretation (summarized in Table 6). Because the object-based method is an objective process, meaning there is little opportunity for human error and no dependence on the varying knowledge and expertise of each interpreter, this method produces more consistent and repeatable results that can be used to accurately compare data from different sources and over time (Morgan et al. 2010). The manual method, however, is strongly dependent on the interpreter, and when multiple interpreters are working on a project they may not have the same level of accuracy, leading to inconsistent output. In addition, once the appropriate user defined segmentation parameters are determined for an image, they can be directly applied to various images with similar land cover, making this process even more consistent and efficient. A downside of the object-based method is that it has historically required more specialized, and potentially more expensive, software than the manual method. This may act as a barrier preventing the more widespread use of this method; however, this approach is being integrated into more software platforms (e.g., ArcPro) and prices are declining such that it is becoming more readily available (see Marcaccio et al. 2021 for other software examples). The object-based method can also be more computer intensive to create objects than manual delineation, particularly when larger areas need to be delineated. eCognition (the software used herein) does, however, have built-in features designed to apply a similar algorithm across large images by breaking them into subsets in order to mitigate this concern. The software can also use one ruleset and automatically apply it to a large batch of images if they all have similar land cover (Marcaccio and Chow-Fraser 2018).

There have been many successful uses of this object-based processes in the literature, but few studies have actually compared the results of manual delineation and object-based segmentation. The existing studies do, however, indicate promising outcomes with similar results as those presented here including: similar accuracy levels between the two methods (Morgan and Gergel 2013; Kampouraki et al. 2007) and strong agreement between the classifications of the two methods (Zhou and Troy 2008). This study, however, is the first to demonstrate the potential savings in time and effort that the object-based method provides. Given the advantages from an efficiency perspective as well as more precise boundary delineation and comparable overall accuracy, we recommend that object-based segmentation be used where possible to facilitate the accurate interpretation of aerial imagery.

ACKNOWLEDGEMENTS

We are grateful to the Canadian Wildlife Service, Ontario Region, for support and encouragement to undertake this project, particularly support from Greg Grabas, Nancy Patterson, Ian Smith, and Zing-Ying Ho. We also appreciate the input from two reviewers who helped to improve these works and technical editing from Emily Marshall. Funding for this project came from the Canadian Wildlife Service of Environment and Climate Change Canada.

REFERENCES

Benz, U.C., Hofmann, P., Willhauck, G., Lingenfelder, I. and Heynen, M. 2004. Multi-resolution, object-oriented fuzzy analysis of remote sensing data for GIS-ready information. ISPRS Journal of Photogrammetry and Remote Sensing, 58(3-4): 239-258.

Blaschke, T. 2010. Object based image analysis for remote sensing. ISPRS Journal of Photogrammetry and Remote Sensing, 65: 2-16.

Burnett, C., and Blaschke, T. 2003. A multi-scale segmentation/object relationship modeling methodology for landscape analysis. Ecological Modeling, 168: 233-249.

Congalton, R.G. 1991. A review of assessing the accuracy of classification of remotely sensed data. Remote Sensing of Environment, 37: 35-46.

Dauwalter, D.C., Fesenmyer, K.A., Bjork, R., Leasure, D.R. and Wenger, S.J. 2017. Satellite and Airborne Remote Sensing Applications for Freshwater Fisheries. Fisheries, 42: 526-537.

Grenier, M., Labrecque, S., Garneau, M. and Tremblay, A. 2008. Object-based classification of a SPOT-4 image for mapping wetlands in the context of greenhouse gases emissions: The case of the Eastmain region, Québec, Canada. Canadian Journal of Remote Sensing, 34: S398-S413.

Jung, J.A., Rokitnicki-Wojcik, D. and Midwood, J.D. 2017. Characterizing past and modelling future spread of *Phragmites australis* ssp. *australis* at Long Point Peninsula, Ontario, Canada. Wetlands, 37(5): 961-973.

Kampouraki, M., Wood, G.A. and Brewer, T.R. 2007. The suitability of object-based image segmentation to replace manual aerial photo interpretation for mapping impermeable land cover. In: Remote Sensing and Photogrammetry Society Annual Conference (RSPSoc 2007): Challenges for Earth Observation: Scientific, Technical and Commercial, 426-430.

Lee, H.T., Bakowsky, W.D., Riley, J.L., Bowles, J., Puddister, M., Uhlig, P., and McMurray, S. 1998. Ecological Community Classification for Southern Ontario: First Approximation and Its Application. Ontario Ministry of Natural Resources, Southcentral Science Section, Science Development and Transfer Branch. SCSS Field Guide FG-02.

Liu, D. and Yu, J. 2009. Otsu Method and K-means. Ninth International Conference on Hybrid Intelligent Systems, 2009, 344-349.

Marcaccio, J.V. and Chow-Fraser, P., 2018. Mapping invasive Phragmites australis in highway corridors using provincial orthophoto databases in Ontario. Ontario Ministry of Transportation. Technical Report #2015-15.

Marcaccio, J.V., Gardner Costa J., and Midwood J.D. 2021. Potential use of remote sensing to support the management of freshwater fish habitat in

Canada. Canadian Technical Report of Fisheries and. Aquatic Science, 3197: viii + 57 p.

Midwood, J.D. and Chow-Fraser, P. 2010. Mapping floating and emergent aquatic vegetation in coastal wetlands of Eastern Georgian Bay, Lake Huron, Canada. Wetlands, 30(6): 1141-1152.

Morgan, J.L. and Gergel, S.E., 2013. Automated analysis of aerial photographs and potential for historic forest mapping. Canadian Journal of Forest Research, 43(8): 699-710.

Morgan, J.L., Gergel, S.E., and Coops, N.C. 2010. Aerial Photography: A Rapidly Evolving Tool for Ecological Management. Bioscience, 60(1): 47-59.

Pande-Chhetri, R., Abd-Elrahman, A., Liu, T., Morton, J. and Wilhelm, V.L. 2017. Object-based classification of wetland vegetation using very high-resolution unmanned air system imagery. European Journal of Remote Sensing, 50(1): 564-576.

Pettorelli, N., Wegmann, M., Skidmore, A. K., Mucher, S., Dawson, T. P., Fernandez, M., Lucas, R., Schaepman, M.E., Wang, T., O'Connor, B., Jongman, R.H.G., Kempeneers, P., Sonnenschein, R., Leuidner, A.K., Bohm, M., He, K.S., Nagendra, H., Dubois, G., Fatoyinbo, T., Hansen, M.C., Paganini, M., de Klerk, H.M., Asner, G.P., Kerr, J.T., Nestor Fernandez, A.B., Lausch, A., Cho, M.A., Alcaraz-Segura, D., McGeoch, M.A., Turner, W., Mueller, A., St-Louis, V., Penner, J., Vihervaara, P., Belward, A., Reyers, B., and Geller, G. N. 2016. Framing the concept of satellite remote sensing essential biodiversity variables: challenges and future directions. Remote Sensing in Ecology and Conservation, 122–131.

Pringle, R.M., Syfert, M., Webb, J.K. and Shine, R. 2009. Quantifying historical changes in habitat availability for endangered species: use of pixel-and object-based remote sensing. Journal of Applied Ecology, 46(3): 544-553.

R Core Team. 2020. R: A language and environment for statistical computing. R Foundation for Statistical Computing, Vienna, Austria. URL https://www.R-project.org/.

Thompson, I.D., Maher, S.C., Rouillard, D.P., Fryxell, J.M., and Baker, J.A. 2007. Accuracy of forest inventory mapping: some implications for boreal forest management. Forest Ecology and Management, 252(1–3): 208-221.

Wulder, M. 1998. Optical remote sensing techniques for the assessment of forest inventory and biophysical parameters. Progress in Physical Geography, 22: 449-476.

Wulder, M., White, J.C., Hay, G.J., and Castilla, G. 2008. Towards automated segmentation of forest inventory polygons on high spatial resolution satellite imagery. The Forestry Chronicle, 84(2): 221–230.

Zhou, W., and Troy, A. 2008. An object-oriented approach for analyzing and characterizing urban landscape at the parcel level. International Journal of Remote Sensing, 29(11): 3119-3135.

Table 1: Descriptions of the nine land cover classes that were delineated in this study along with their class code and examples of representative species.

Class Code	Class Name	Description	Representative Genus/Genera*
MA	Shallow Marsh	Hydrophytic emergent plant (>25% cover) dominated with less than 25% tree and shrub cover.	Cattail (*Typha sp*) Bulrush (*Schoenoplectus sp.*) Spike-rush (*Eleocharis sp.*) Arrowhead (*Sagittaria sp.*) Bur-reed (*Sparganium sp.*)
CMA**	Cattail Marsh	Cattail dominated shallow marsh	Cattail (*Typha sp.*);
BMA**	Bulrush Marsh	Bulrush dominated shallow marsh	Bulrush (*Schoenoplectus sp.*)
MME	Mixed Meadow	Mix of grass-like (e.g. grass and sedge) and broadleaf species (e.g. forbs).	Reedgrass (*Calamagrostis sp.*) Sedge (*Carex sp.*) Anemone (*Anemone* sp.)
PHG	Phragmites	Non-native Common Reed *Phragmites australis* subsp. *australis* dominated with scattered herbaceous species.	Reed *(Phragmites sp.)*
ESA	Emergent Shallow Aquatic	Scattered or patchy emergent dominated class (5-25%) in aquatic areas.	Cattail (*Typha sp.*) Bulrush (*Schoenoplectus sp.*)
FSA	Floating-leaved Shallow Aquatic	Floating-leaved macrophyte dominated (>25%) aquatic areas.	Pond lily (*Nuphar sp*.) Waterlily (*Nymphaea sp*.)
Water	Open Water	Mix of open water (<25% submerged macrophytes) and submerged macrophytes (>25%). No tree or shrub cover and very low emergent cover (<5%).	Waterweed (*Elodea sp.*) Pondweed (*Potamogeton sp.*) Naiad (*Najas sp.*)
Other	Other	All other land cover types not targeted by the study; typically representing forest.	N/A

*Based on field-based vegetation surveys conducted at the site for other studies and projects.
**Represent two marsh sub-types that reflect the dominant emergent species.

Table 2: Total time required to complete all components of the manual delineation and object-based segmentation methods in minutes. Asterisks (*) identify the interpretation method that was completed first for each subset.

	Manual Delineation				Object-Based Segmentation				
	Start Editing	Complete delineation and classification	Merge polygons	Total Time	Run object-based segmentation	Complete classification	Complete Export	Complete Import into ArcMap	Total Time
Subset 1	0.03	40.53	2.27	*42.83	0.68	28.27	0.05	0.03	29.02
Subset 2	0.04	70.48	3.47	73.99	0.68	40.57	0.04	0.02	*41.32
Subset 3	0.03	38.17	2.87	*41.06	0.77	17.08	0.04	0.02	17.92
Subset 4	0.04	51.27	3.57	54.87	0.80	24.15	0.04	0.02	*25.00
Subset 5	0.06	54.92	4.02	*59.00	0.68	35.12	0.06	0.02	35.88
Subset 6	0.03	34.20	2.97	37.20	0.66	19.02	0.06	0.02	*19.75
Subset 7	0.03	28.80	3.27	*32.10	0.69	14.33	0.04	0.02	15.09
Subset 8	0.03	45.42	3.78	49.23	0.69	23.97	0.04	0.02	*24.72
Subset 9	0.04	88.03	4.42	*92.49	0.66	44.83	0.08	0.01	45.59
Subset 10	0.03	58.63	3.77	62.43	0.51	27.50	0.06	0.02	*28.09
Mean Time	0.04	51.05	3.44	54.52	0.68	27.48	0.05	0.02	28.24

Table 3: Number of cursor clicks required to complete the interpretation of each image subset using the manual delineation and object-based segmentation methods. The number of vertices in polygons created by the object-based method and the number of polygons created by both methods are also shown. The number of vertices in polygons created by the manual method is equal to the number of cursor clicks.

Method	Subset 1	Subset 2	Subset 3	Subset 4	Subset 5	Subset 6	Subset 7	Subset 8	Subset 9	Subset 10	Mean	Standard Deviation
Number of Cursor Clicks – Manual Delineation	6,623	3,435	7,604	10,166	11,370	6,982	7,018	9,476	14,418	11,433	8,853	3,142
Number of Cursor Clicks – Object-Based Segmentation	647	809	552	594	772	504	445	633	788	600	634	123
Number of Vertices in Object-Based Polygons	34,787	71,160	31,473	42,994	58,897	35,912	26,105	40,221	66,692	49,366	45,761	15,330
Number of Polygons in Manual Delineation	41	59	42	51	61	38	41	49	86	59	53	14
Number of Polygons in Object-Based Segmentation	53	148	61	81	118	75	69	93	161	108	97	36

Table 4: Overall agreement between classifications assigned by each method and the classifications of reference points statistic for each method.

Subset	Manual Delineation	Object-Based Segmentation
	Overall Agreement (%)	Overall Agreement (%)
1	92	91
2	88	90
3	94	95
4	89	93
5	87	82
6	88	91
7	91	90
8	91	89
9	94	88
10	92	90
Mean	91	90
Standard Deviation	2.50	3.41

Table 5: Mean user and producer accuracy of classifications by manual delineation and object-based segmentation for each land cover class.

Class	Manual Delineation		Object-Based Segmentation	
	Mean User Accuracy (%)	Mean Producer Accuracy (%)	Mean User Accuracy (%)	Mean Producer Accuracy (%)
MA	86	84	89	91
CMA	58	88	72	93
BMA	54	45	84	48
MME	89	89	87	78
Other	100	50	100	50
Water	94	93	100	93
ESA	70	87	91	81
FSA	56	100	100	80
PHG	81	80	50	100

Table 6: Summary of the advantages and disadvantages of the object-based segmentation method and the manual delineation method of aerial image interpretation.

Method	Advantages	Disadvantages
Object-Based Segmentation	- faster - less labour intensive - objective - less opportunity for human error in boundary delineation - consistent and repeatable results - precise boundary delineation	- cannot incorporate logical decisions - identifies objects/polygons, not real objects - requires specialized and expensive software
Manual Delineation	- incorporates logical decisions - identifies real objects, not object-based interpretations - widely used method	- time consuming - labour intensive - subjective - opportunity for human error - inconsistent results - imprecise boundary delineation

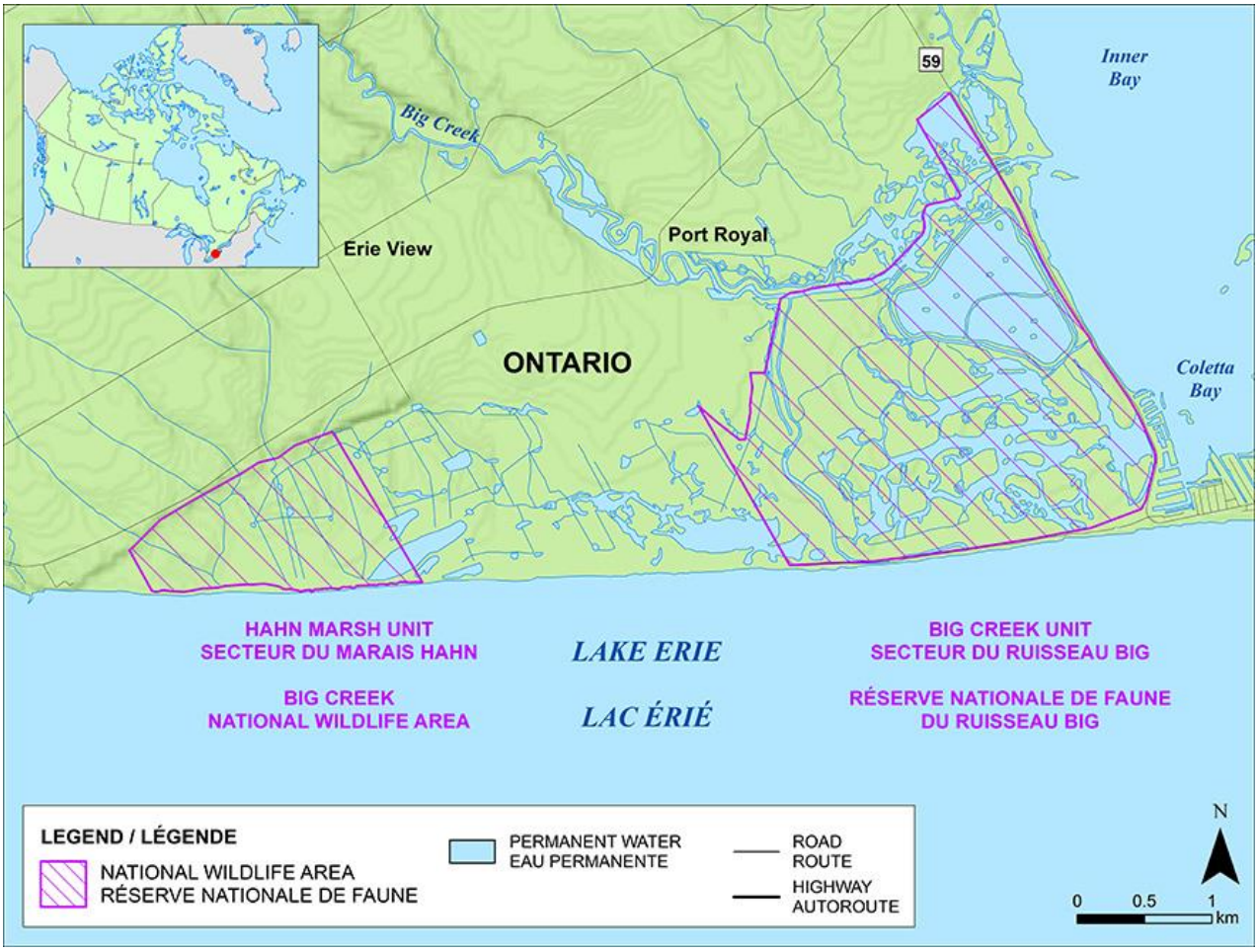

Figure 1: Location of Big Creek National Wildlife Area (managed by Environment and Climate Change Canada) in Canada (red dot in inset) and near Port Royal, Ontario.

Figure 2: Locations of ten image subsets within the study site, the Big Creek Unit of Big Creek National Wildlife Area (SWOOP 2006).

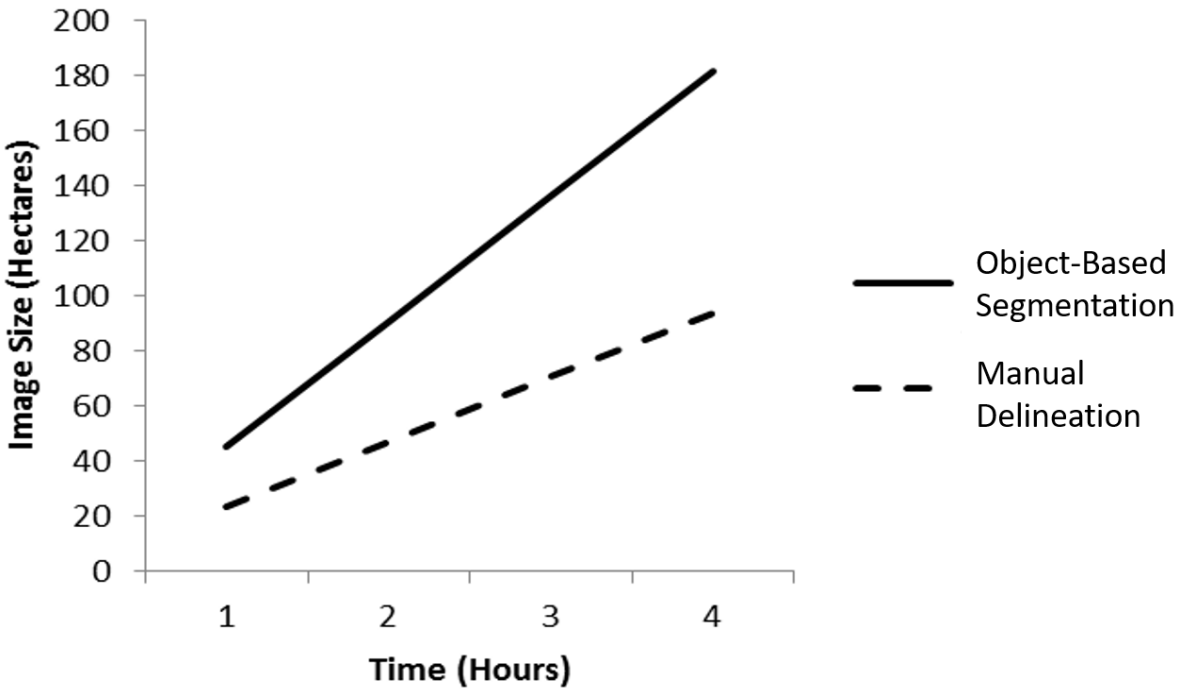

Figure 3: Predicted time required to interpret various image sizes using the manual delineation and object-based segmentation methods.

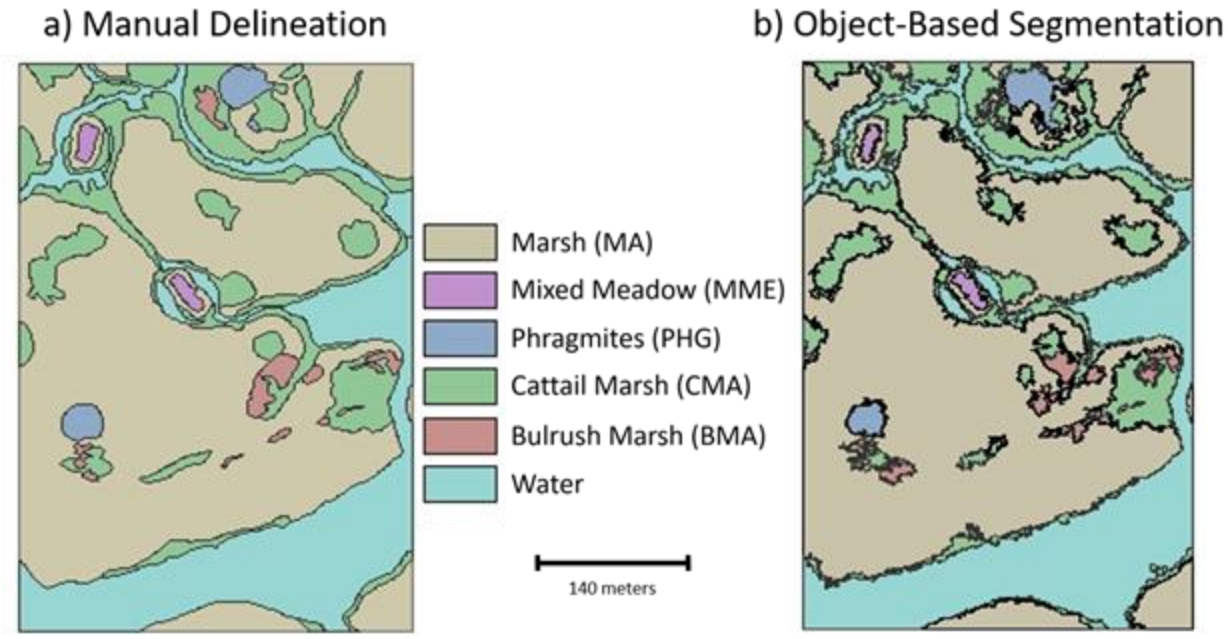

Figure 4: Comparison of the areas classified as each land cover type by manual delineation and object-based segmentation. Image a) was created by manual delineation and image b) was created by object-based segmentation.

a) Manual Delineation

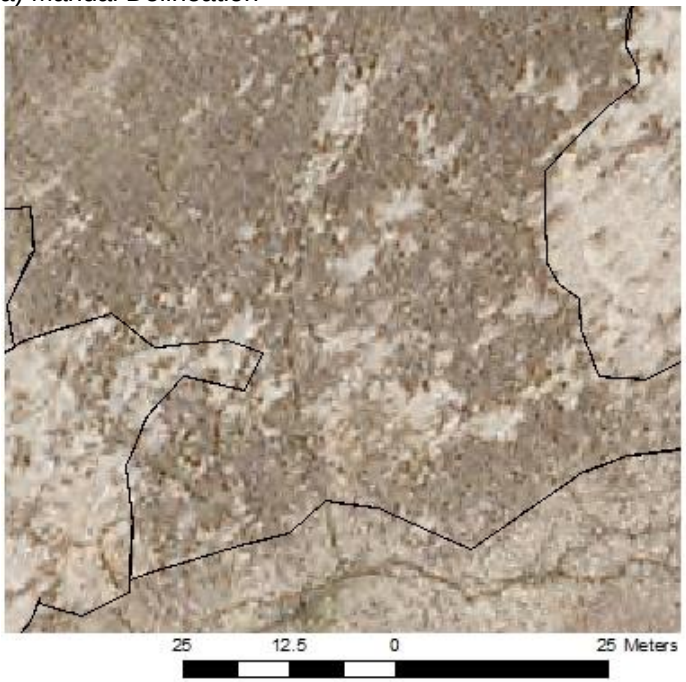

b) Object-Based Segmentation

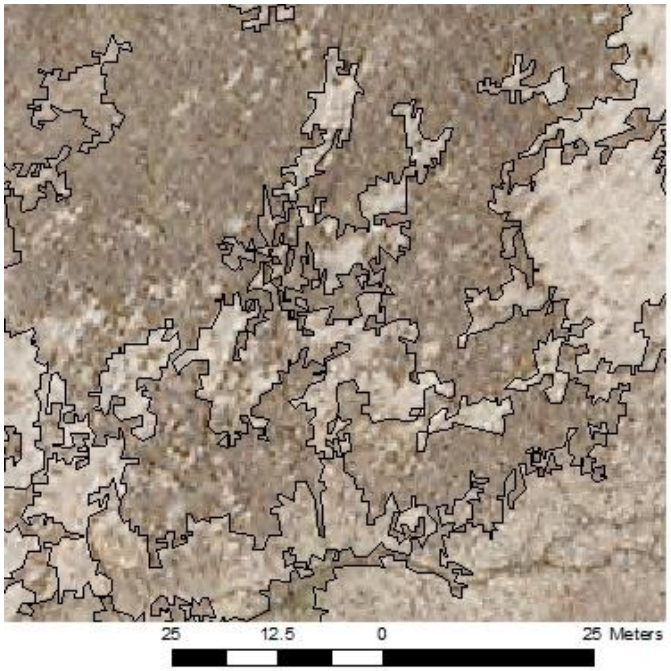

Figure 5: An example of the shallow marsh landscape patterns where Cattail Marsh (CMA) and Bulrush Marsh (BMA) land class delineations are shown. Image a) was created by manual delineation and image b) was created by object-based segmentation.

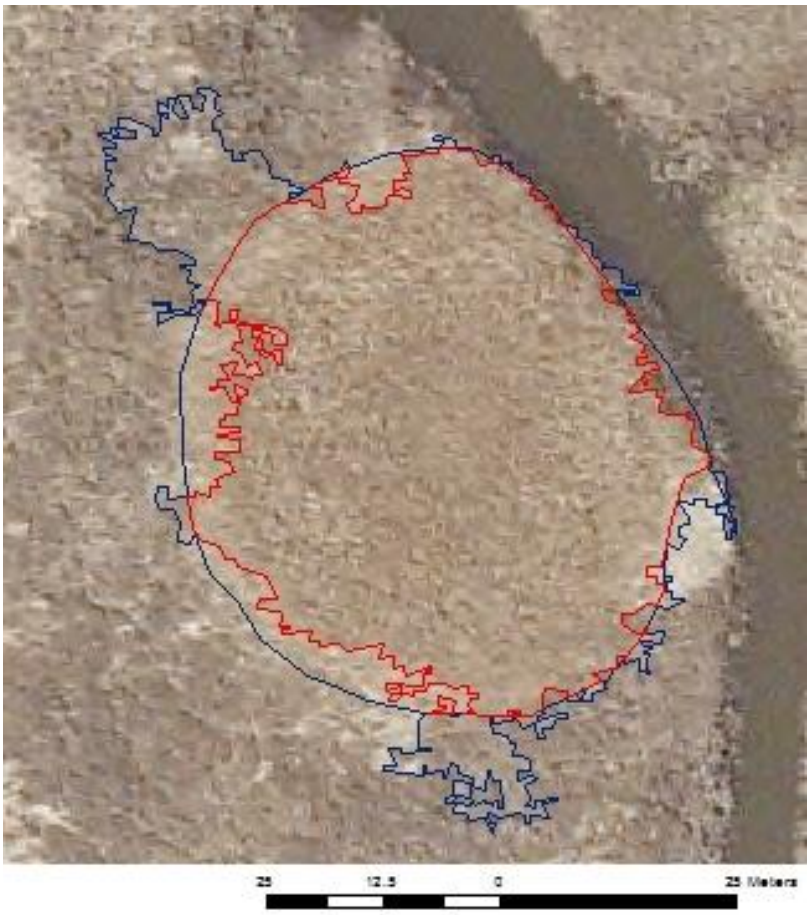

Figure 6: Example of a Phragmites (PHG) patch that was delineated with the object-based segmentation and manual delineation methods. The area classified as PHG in agreement between the two methods is outlined in red. Areas that were not classified as PHG in agreement between the methods are outlined in blue.

Figure 7: Red polygons were not assigned land cover classifications in agreement between the two methods. The majority of inconsistently classified polygons are located along feature boundaries, indicating the differences in boundary precision of the two methods, or near Cattail Marsh (CMA) and Bulrush Marsh (BMA) patches.

APPENDIX A – CONFUSION MATRICES FOR CLASSIFICATION ACCURACY

These confusion matrices (or contingency tables) show the number of random reference points that were correctly classified into each land cover type. The producer's accuracy describes the number of reference points correctly classified on the map (inverse of omission error), and the user's accuracy describes the number of correctly classified points for that land cover type (inverse of commission error).

Table A1: Subset 1 manual delineation confusion matrix.

Land Cover in Image	Land Cover of Reference Points									Row Total	User Accuracy (%)
	MA	CMA	BMA	MEM	Other	Water	ESA	FSA	PHG		
MA	61									61	100
CMA	4	6	1							11	55
BMA		1	5							6	83
MME	1			2						3	67
Other											
Water						15				15	100
ESA											
FSA	1							3		4	75
PHG											
Column Total	67	7	6	2		15		3		100	
Producer Accuracy (%)	91	85	83	100		100		100			

Overall Agreement: 92%

Table A2: Subset 1 object-based segmentation confusion matrix.

Land Cover in Image	Land Cover of Reference Points									Row Total	User Accuracy (%)
	MA	CMA	BMA	MME	Other	Water	ESA	FSA	PHG		
MA	60			1						61	98
CMA	3	8								11	72
BMA	1	2	3							6	50
MME	1			1				1		3	33
Other											
Water						15				15	100
ESA											
FSA								4		4	100
PHG											
Column Total	65	10	3	2		15		5		100	
Producer Accuracy (%)	92	80	100	50		100		80			

Overall Agreement: 91%

Table A3: Subset 2 manual delineation confusion matrix.

Land Cover in Image	Land Cover of Reference Points									Row Total	User Accuracy (%)
	MA	CMA	BMA	MME	Other	Water	ESA	FSA	PHG		
MA	48									48	100
CMA	2	18								20	90
BMA	6	3	14							23	60
MME				1						1	100
Other					3					3	100
Water						3				3	100
ESA											
FSA											
PHG	1								1	2	50
Column Total	57	21	14	1	3	3			1	100	
Producer Accuracy (%)	84	85	100	100	100	100			100		

Overall Agreement: 88%

Table A4: Subset 2 object-based segmentation confusion matrix.

Land Cover in Image	Land Cover of Reference Points									Row Total	User Accuracy (%)
	MA	CMA	BMA	MME	Other	Water	ESA	FSA	PHG		
MA	46	1		1						48	95
CMA	2	19								21	90
BMA	2	1	19							22	86
MME				1						1	100
Other					3					3	100
Water						3				3	100
ESA											
FSA											
PHG	2									2	0
Column Total	52	21	19	2	3	3				100	
Producer Accuracy (%)	88	90	100	50	100	100					

Overall Agreement: 91%

Table A5: Subset 3 manual delineation confusion matrix.

Land Cover in Image	Land Cover of Reference Points									Row Total	User Accuracy (%)
	MA	CMA	BMA	MME	Other	Water	ESA	FSA	PHG		
MA	74	1								75	99
CMA	2	8				2				12	67
BMA											
MME				1						1	100
Other											
Water		1				11				12	92
ESA											
FSA											
PHG											
Column Total	76	10		1		13				100	
Producer Accuracy (%)	97	80		100		85					

Overall Agreement: 94%

Table A6: Subset 3 object-based segmentation confusion matrix.

Land Cover in Image	Land Cover of Reference Points									Row Total	User Accuracy (%)
	MA	CMA	BMA	MME	Other	Water	ESA	FSA	PHG		
MA	74	1								75	99
CMA	1	8				3				12	67
BMA											
MME				1						1	100
Other											
Water						12				12	100
ESA											
FSA											
PHG											
Column Total	75	9		1		15				100	
Producer Accuracy (%)	99	89		100		80					

Overall Agreement: 95%

Table A7: Subset 4 manual delineation confusion matrix.

Land Cover in Image	Land Cover of Reference Points									Row Total	User Accuracy (%)
	MA	CMA	BMA	MME	Other	Water	ESA	FSA	PHG		
MA	49	2	2							53	92
CMA	3	13	2			2				20	65
BMA											
MME				1						1	100
Other											
Water						23				23	100
ESA											
FSA											
PHG									3	3	100
Column Total	52	15	4	1		25			3	100	
Producer Accuracy (%)	94	87	0	100		92			100		

Overall Agreement: 89%

Table A8: Subset 4 object-based segmentation confusion matrix.

Land Cover in Image	Land Cover of Reference Points									Row Total	User Accuracy (%)
	MA	CMA	BMA	MME	Other	Water	ESA	FSA	PHG		
MA	49		4							53	92
CMA	3	17								20	85
BMA											
MME				1						1	100
Other											
Water						23				23	100
ESA											
FSA											
PHG									3	3	100
Column Total	52	17	4	1		23			3	100	
Producer Accuracy (%)	94	100	0	100		100			100		

Overall Agreement: 93%

Table A9: Subset 5 manual delineation confusion matrix.

Land Cover in Image	Land Cover of Reference Points									Row Total	User Accuracy (%)
	MA	CMA	BMA	MME	Other	Water	ESA	FSA	PHG		
MA	18	1								19	95
CMA	3	31	2				2			38	82
BMA		2	1							3	33
MME		1		4						5	80
Other											
Water						26				26	100
ESA						2	6			8	75
FSA											
PHG									1	1	100
Column Total	21	35	3	4		28	8		1	100	
Producer Accuracy (%)	86	89	33	100		93	75		100		

Overall Agreement: 87%

Table A10: Subset 5 object-based segmentation confusion matrix.

Land Cover in Image	Land Cover of Reference Points									Row Total	User Accuracy (%)
	MA	CMA	BMA	MME	Other	Water	ESA	FSA	PHG		
MA	18		1							19	95
CMA	8	25	4				1			38	66
BMA			3							3	100
MME		2		3						5	60
Other											
Water						26				26	100
ESA						1	7			8	88
FSA											
PHG		1								1	0
Column Total	26	28	8	3		27	8			100	
Producer Accuracy (%)	69	89	38	100		96	88				

Overall Agreement: 82%

Table A11: Subset 6 manual delineation confusion matrix.

Land Cover in Image	Land Cover of Reference Points									Row Total	User Accuracy (%)
	MA	CMA	BMA	MME	Other	Water	ESA	FSA	PHG		
MA	54		2						1	57	95
CMA	5	22			1	2				30	73
BMA											
MME											
Other											
Water		1				12				13	92
ESA											
FSA											
PHG											
Column Total	59	23	2		1	14			1	100	
Producer Accuracy (%)	92	96	0		0	86			0		

Overall Agreement: 88%

Table A12: Subset 6 object-based segmentation confusion matrix.

Land Cover in Image	Land Cover of Reference Points									Row Total	User Accuracy (%)
	MA	CMA	BMA	MME	Other	Water	ESA	FSA	PHG		
MA	55	1	1							57	96
CMA	4	23			1	2				30	77
BMA											
MME											
Other											
Water						13				13	100
ESA											
FSA											
PHG											
Column Total	59	24	1		1	15				100	
Producer Accuracy (%)	93	96	0		0	87					

Overall Agreement: 91%

Table A13: Subset 7 manual delineation confusion matrix.

Land Cover in Image	Land Cover of Reference Points									Row Total	User Accuracy (%)
	MA	CMA	BMA	MME	Other	Water	ESA	FSA	PHG		
MA	41	2								43	95
CMA	4	7				3				14	50
BMA											
MME											
Other											
Water						43				43	100
ESA											
FSA											
PHG											
Column Total	45	9				46				100	
Producer Accuracy (%)	91	78				93					

Overall Agreement: 91%

Table A14: Subset 7 object-based segmentation confusion matrix.

Land Cover in Image	Land Cover of Reference Points									Row Total	User Accuracy (%)
	MA	CMA	BMA	MME	Other	Water	ESA	FSA	PHG		
MA	42					1				43	98
CMA	4	5				5				14	36
BMA											
MME											
Other											
Water						43				43	100
ESA											
FSA											
PHG											
Column Total	46	5				49				100	
Producer Accuracy (%)	91	100				88					

Overall Agreement: 90%

Table A15: Subset 8 manual delineation confusion matrix.

Land Cover in Image	Land Cover of Reference Points									Row Total	User Accuracy (%)
	MA	CMA	BMA	MME	Other	Water	ESA	FSA	PHG		
MA	9	1	1							11	82
CMA		22		2			1			25	88
BMA											
MME				3						3	100
Other											
Water						32				32	100
ESA						4	25			29	86
FSA											
PHG											
Column Total	9	23	1	5		36	26			100	
Producer Accuracy (%)	100	96	0	60		89	96				

Overall Agreement: 91%

Table A16: Subset 8 object-based segmentation confusion matrix.

Land Cover in Image	Land Cover of Reference Points									Row Total	User Accuracy (%)
	MA	CMA	BMA	MME	Other	Water	ESA	FSA	PHG		
MA	10	1								11	91
CMA		18		1		1	5			25	72
BMA											
MME				3						3	100
Other										0	
Water						32				32	100
ESA						3	26			29	90
FSA											
PHG											
Column Total	10	19		4		36	31			100	
Producer Accuracy (%)	100	95		75		89	84				

Overall Agreement: 89%

Table A17: Subset 9 manual delineation confusion matrix.

Land Cover in Image	Land Cover of Reference Points									Row Total	User Accuracy (%)
	MA	CMA	BMA	MME	Other	Water	ESA	FSA	PHG		
MA	2			1						3	67
CMA		57				1	2			60	95
BMA											
MME				1						1	100
Other											
Water						17				17	100
ESA		2					17			19	89
FSA											
PHG											
Column Total	2	59		2		18	19			100	
Producer Accuracy (%)	100	97		50		94	89				

Overall Agreement: 94%

Table A18: Subset 9 object-based segmentation confusion matrix.

Land Cover in Image	Land Cover of Reference Points									Row Total	User Accuracy (%)
	MA	CMA	BMA	MME	Other	Water	ESA	FSA	PHG		
MA	1	1		1						3	33
CMA		50				1	8			59	85
BMA											
MME				1						1	100
Other											
Water						17				17	100
ESA		1					19			20	95
FSA											
PHG											
Column Total	1	52		2		18	27			100	
Producer Accuracy (%)	100	96		50		94	70				

Overall Agreement: 88%

Table A19: Subset 10 manual delineation confusion matrix.

Land Cover in Image	Land Cover of Reference Points									Row Total	User Accuracy (%)
	MA	CMA	BMA	MME	Other	Water	ESA	FSA	PHG		
MA	49									49	100
CMA	5	23								28	82
BMA			1							1	100
MME				2						2	100
Other											
Water		3				16				19	84
ESA											
FSA											
PHG									1	1	100
Column Total	54	26	1	2		16			1	100	
Producer Accuracy (%)	91	88	100	100		100			100		

Overall Agreement: 92%

Table A20: Subset 10 object-based segmentation confusion matrix.

Land Cover in Image	Land Cover of Reference Points									Row Total	User Accuracy (%)
	MA	CMA	BMA	MME	Other	Water	ESA	FSA	PHG		
MA	47	1	1							49	96
CMA	7	20				1				28	71
BMA			1							1	100
MME				2						2	100
Other											
Water						19				19	100
ESA											
FSA											
PHG									1	1	100
Column Total	54	21	2	2		20			1	100	
Producer Accuracy (%)	87	95	50	100		95			100		

Overall Agreement: 90%

APPENDIX B – CONFUSION MATRICES FOR LAND COVER AREA

Table B1: Area classified as each land cover type in subset 1 (m^2).

Manual Delineation	Object-Based Segmentation									Row Total	Proportional Area Overlap
	MA	CMA	BMA	MME	Other	Water	ESA	FSA	PHG		
MA	127622	3993	2045	2400		873		1158	49	138139	0.92
CMA	2111	18205	1104			140				21561	0.84
BMA	287	601	6683	15					6	7592	0.88
MME	467		29	2353		2		288		3139	0.75
Other											
Water	461	231		5		32496		323		33517	0.97
ESA											
FSA	38					432		8446		8916	0.95
PHG	19		9						319	347	0.92
Blank	0							1		1	
Column Total	131005	23030	9872	4772		33943		10216	373	213211	
Proportional Area Overlap	0.97	0.79	0.68	0.49		0.96		0.83	0.85		

Table B2: Area classified as each land cover type in subset 2 (m^2).

Manual Delineation	Object-Based Segmentation									Row Total	Proportional Area Overlap
	MA	CMA	BMA	MME	Other	Water	FSA	PHG	Blank		
MA	114448	6756	9623	241	218	299		330		131914	0.87
CMA	5667	27940	2401		77	514			0	36599	0.76
BMA	5162	1229	27423					41		33854	0.81
MME	420			347				90		857	0.41
Other	243	126			3434	108		83	0	3995	0.86
Water	14	358			264	2927				3562	0.82
ESA											
FSA											
PHG	825	45	34					1730		2633	0.66
Blank	0	0	0		0	0				1	
Column Total	126779	36454	39480	588	3994	3847		2274	0	213416	
Proportional Area Overlap	0.90	0.77	0.69	0.59	0.86	0.76		0.76			

Table B3: Area classified as each land cover type in subset 3 (m^2).

Manual Delineation	Object-Based Segmentation									Row Total	Proportional Area Overlap
	MA	CMA	BMA	MME	Other	Water	ESA	FSA	PHG		
MA	150293	3819	1088	201		654	70		0	156125	0.96
CMA	4659	16019	69			2548	110			23405	0.68
BMA	900	46	1710							2656	0.64
MME	20			521						541	0.96
Other											
Water	150	1523		4		30226				31903	0.95
ESA	1	38				96	669			805	0.83
FSA											
PHG	98								265	363	0.73
Column Total	156121	21446	2867	726		33524	849		265	215799	
Proportional Area Overlap	0.96	0.75	0.60	0.72		0.90	0.79		1.00		

Table B4: Area classified as each land cover type in subset 4 (m^2).

Manual Delineation	Object-Based Segmentation									Row Total	Proportional Area Overlap
	MA	CMA	BMA	MME	Other	Water	ESA	FSA	PHG		
MA	117694	4836	973	117		356			184	124159	0.95
CMA	4782	27258	614			1911			690	35255	0.77
BMA	1007	516	1762			5				3289	0.54
MME	193			917						1109	0.83
Other											
Water	73	1641		0		44991				46705	0.96
ESA											
FSA											
PHG	289	95							2329	2712	0.86
Column Total	124037	34345	3349	1034		47263			3203	213230	
Proportional Area Overlap	0.95	0.79	0.53	0.89		0.95			0.73	0.95	

Table B5: Area classified as each land cover type in subset 5 (m^2).

Manual Delineation	Object-Based Segmentation									Row Total	Proportional Area Overlap
	MA	CMA	BMA	MME	Other	Water	ESA	FSA	PHG		
MA	44425	3257	935	216		65	4		158	49061	0.91
CMA	5880	69000	2391	1168		2040	458		734	81670	0.84
BMA	524	1271	5139	54		45			25	7057	0.73
MME	3	887	69	2562		72				3592	0.71
Other											
Water	116	1183	54	687		45747	1506		54	49347	0.93
ESA	0	1136		3		4186	12598			17924	0.70
FSA											
PHG	151	770	3	92		14			4208	5238	0.80
Column Total	51098	77503	8591	4783		52169	14565		5180	213889	
Proportional Area Overlap	0.87	0.89	0.60	0.54		0.88	0.86		0.81		

Table B6: Area classified as each land cover type in subset 6 (m^2).

Manual Delineation	Object-Based Segmentation									Row Total	Proportional Area Overlap
	MA	CMA	BMA	MME	Other	Water	ESA	FSA	PHG		
MA	119516	6202	1152		58	27			102	127057	0.94
CMA	4383	25280	47		171	1377			4	31261	0.81
BMA	1107	75	2214							3396	0.65
MME											
Other	141	72			955					1168	0.82
Water	8	1155				46004				47166	0.98
ESA											
FSA											
PHG	429	3							2730	3163	0.86
Column Total	125583	32787	3413		1184	47408			2836	213211	
Proportional Area Overlap	0.95	0.77	0.65		0.81	0.97			0.96		

Table B7: Area classified as each land cover type in subset 7 (m^2).

Manual Delineation	Object-Based Segmentation									Row Total	Proportional Area Overlap
	MA	CMA	BMA	MME	Other	Water	ESA	FSA	PHG		
MA	80927	2735		102		137			279	84180	0.96
CMA	2229	16999		3		1219				20448	0.83
BMA											
MME	53	1		603						657	0.92
Other											
Water	355	1546		4		104312				106217	0.98
ESA											
FSA											
PHG	457								1252	1709	0.73
Column Total	84021	21281		711		105667			1531	213211	
Proportional Area Overlap	0.96	0.80		0.85		0.99			0.82		

Table B8: Area classified as each land cover type in subset 8 (m^2).

Manual Delineation	Object-Based Segmentation									Row Total	Proportional Area Overlap
	MA	CMA	BMA	MME	Other	Water	ESA	FSA	PHG		
MA	27122	1863	80	312		312				29690	0.91
CMA	3488	41027	183	436		1583	4891			51607	0.79
BMA	28	72	517							617	0.84
MME	468	510		4495		9	24			5507	0.82
Other											
Water	550	1408		70		62481	5635			70145	0.89
ESA		1163				3956	52710			57830	0.91
FSA											
PHG											
Column Total	31656	46045	780	5314		68341	63260			215395	
Proportional Area Overlap	0.86	0.89	0.66	0.85		0.91	0.83			0.91	

Table B9: Area classified as each land cover type in subset 9 (m^2).

Manual Delineation	Object-Based Segmentation									Row Total	Proportional Area Overlap
	MA	CMA	BMA	MME	Other	Water	ESA	FSA	PHG		
MA	5505	1095		104		210	0			6914	0.80
CMA	1076	82330		375	274	3433	12186	44		99718	0.83
BMA											
MME	465	590		2487		7	1			3549	0.70
Other		18			677	10	149			854	0.79
Water	150	2403		114	115	47689	3513	269		54254	0.88
ESA	3	4547		6	5	1885	42030	32		48509	0.87
FSA		10			0	12	28	370		419	0.88
PHG											
Column Total	7199	90993		3086	1071	53247	57906	715		214216	
Proportional Area Overlap	0.76	0.90		0.81	0.63	0.90	0.73	0.52			

Table B10: Area classified as each land cover type in subset 10 (m^2).

Manual Delineation	Object-Based Segmentation									Row Total	Proportional Area Overlap
	MA	CMA	BMA	MME	Other	Water	ESA	FSA	PHG		
MA	110041	9779	393	173		540			324	121249	0.91
CMA	4898	33822	214	15		2175			0	41125	0.82
BMA	488	336	2288							3112	0.74
MME	118	308		1250						1677	0.75
Other											
Water	114	1622		20		42885				44642	0.96
ESA											
FSA											
PHG	123								1361	1483	0.92
Column Total	115783	45868	2894	1458		45600			1685	213288	
Proportional Area Overlap	0.95	0.74	0.79	0.86		0.94			0.81	0.94	